

**MODELLING AND VIBRATION ANALYSIS OF  
ALVEOLAR RESONANCE MECHANISM OF  
ULTRASOUND-INDUCED  
LUNG HAEMORRHAGE**

**By**

**JOHN JABARAJ A/L DEVADASON**

**Thesis submitted in fulfilment of the requirements  
for the degree of  
Doctor of Philosophy**

**OCTOBER 2013**

## ACKNOWLEDGEMENTS

In the late 2009, I was accepted into the Ph.D. program of the Department of Medical Physics, School of Physics, Universiti Sains Malaysia; to study the bioeffect of ultrasound in lungs. My Ph.D. supervisor is Prof. Dr. Mohamad Suhaimi Jaafar; a flexible, humble and knowledgeable professor, who plotted the course of my studies with well given advices and encouragements. Thus, I thank him profusely and I owe him much for the completion of my research and the production of this thesis. My Ph.D. studies and I are sponsored by the MSI-Universiti Kuala Lumpur through its further education scheme. Hence, I will be forever indebted to the institution for the opportunity given.

During the long hard years of academic studies, one must not live in a cocoon and forget the outside world. Studies are important but are not everything. Therefore amidst studies, I somehow managed to meet a sweet fiery nurse from a hospital nearby the university. After months of wooing I convinced her to get married (or was it the other way around...). Here I would like to thank my wonderful and pretty wife, Suganthi Maria, for bringing joy to my heart and meaning to my earthly life. I also thank her for baby *Purple*.

The foundations of a person's character and obsessions begin at home. Thus I thank and honour my parents, Periathai Darling and Devadason Seeni for raising me up rightly and giving me an undying thirst for knowledge by filling up the home with books and throwing away the idiot box. Furthermore, I would like to thank all my

dear brothers and sisters for taking care of me and supporting me while growing up together.

At the end of the day, a scientist filled with knowledge must never become egoistical, proud and starts doubting and questioning GOD. This is foolish and he/she lacks wisdom for knowledge is not created by humans but comes from GOD. Hence I, D. John Jabaraj; bow humbly and give everlasting praises and ultimate thanks to my Lord, Creator and Redeemer; the One and Only, Jesus Christ.

*For Sugarykutty and baby Purple...*

## TABLE OF CONTENTS

	Pg.
Acknowledgements	ii
Table of Contents	iv
List of Tables	viii
List of Figures	ix
List of Symbols	xiii
List of Abbreviations	xvi
Abstrak	xvii
Abstract	xix
<b>CHAPTER 1 – INTRODUCTION</b>	
1.1 Research Background	1
1.2 Research Problem	3
1.3 Objectives of Study	4
1.4 Scope of Study	5
1.5 Outline of Thesis	5
<b>CHAPTER 2 – LITERATURE REVIEW AND THEORY</b>	
2.1 Literature Review	7
2.1.1 The Bioeffects of Ultrasound	7
2.1.2 The Ultrasound-Induced Lung Haemorrhage	9
2.1.3 Inertial Cavitations Mechanism	13

2.1.4 Alveolar Resonance Mechanism	15
2.1.5 The Alveoli	16
2.1.5.1 Function of Alveoli	16
2.1.5.2 Structure of Alveolus	17
2.1.5.3 Alveolar Wall	19
2.1.5.4 Strain in Alveolar Wall	20
2.1.6 Risk Indicators of Ultrasound Bioeffects	21
2.2 Theory	22
2.2.1 Ultrasound Characteristics	22
2.2.2 Propagation Modes of Waves	23
2.2.3 Modelling and Vibration Analysis	25
2.2.4 The Two-Dimensional Wave Equation	29
2.2.5 Forced Vibration by Acoustic Wave	31
2.2.6 The Forced Vibration of Single Degree-of-Freedom System	31
2.2.7 The Q-factor	35
2.2.8 Areal Strain	36
 <b>CHAPTER 3 – METHODOLOGY</b>	
3.1 The Process of Modelling and Vibration Analysis	37
3.2 The Modelling of Alveolar Structure	39
3.3 Derivation of Equations of Resonant Frequency	42
3.3.1 The Square Membrane Model	42
3.3.2 The Circular Membrane Model	45
3.3.3 Transverse Wave Velocity	50
3.3.4 The Added Virtual Mass Increment	52

3.4	Forced Vibration of Membrane Models	53
3.4.1	The Equations of Q-factor	55
3.4.2	The Equations of Equivalent Area Density	56
3.4.3	Areal Strain of Resonance at Fundamental Mode	57
3.4.4	Derivation of Threshold Pressure Equations	60
3.5	The Dimensions of Alveolar Wall Facet of Adult Mammals and Human	63

## **CHAPTER 4 – RESULTS AND DISCUSSION**

4.1	Analysis of Resonant Frequency of Membrane Models	67
4.1.1	Transverse Wave Velocity	67
4.1.2	Utilization of Fundamental Frequency Equations	69
4.1.3	The AVMI Factor Calculation	76
4.1.4	Sample Calculation of Resonant Frequencies	77
4.2	Analysis of Forced Vibration of Membrane Models	79
4.2.1	Amplitude of Forced Vibration	79
4.2.2	The Q-factor Calculation	84
4.2.3	The Deflection at Fundamental Mode	85
4.2.4	Utilization of Threshold Pressure Equations	88
4.3	Validation of Theoretical Study of Alveolar Resonance Mechanism	88
4.4	Construction of Invalidation Experiment	96
4.5	Theoretical Predictions and Comparison with Past Studies	97
4.6	Justification of Modelling Method	103
4.7	Limitations of Assumptions and Approximations	105

	<b>CHAPTER 5 – SUMMARY AND CONCLUSION</b>	<b>107</b>
--	---	------------

<b>REFERENCES</b>	110
<b>APPENDICES</b>	
Appendix A: The forces in vibrating membrane	126
Appendix B: Bending stiffness of alveolar wall facet	128
Appendix C: Equation of elastic tension in membranes	130
Appendix D: The $Q_{medium}$ of alveolar wall facet	131
Appendix E: The $Q_{support}$ of vibrating membranes	132
Appendix F: The areal strain in alveolar wall	134
Appendix G: Dimensions of alveolus in adult mammals and human	135
Appendix H: Introduction to interval arithmetic	136
Appendix I: The threshold pressures (at frequency values) data of the past experimental studies on US-induced lung haemorrhage and of the theoretical study on alveolar resonance mechanism.	137
Appendix J: The ultrasound frequency ranges in medical imaging	141
<b>LIST OF PUBLICATIONS</b>	142

## LIST OF TABLES

		Pg.
Table 3.1	The approximated dimensions of the alveolar wall facet of selected adult mammals and human	65
Table 4.1	The formulas of fundamental frequency of the membrane models of alveolar wall facet for selected adult mammals and human	70
Table 4.2	Maximum values of AVMI factor of the membrane models (at fundamental mode) for selected adult mammals and human	76
Table 4.3	The Q-factor values (at minimum alveolar wall thickness) for the membrane models of alveolar wall facet for selected adult mammals and human	85
Table 4.4	The formulas of threshold pressure for the membrane models of alveolar wall facet for selected adult mammals and human	89
Table 4.5	The chi-square values for membrane models of alveolar wall facet together with the critical chi-square (0.05 significance) for the adult mouse and rat	95
Table 4.6	Predicted theoretical threshold pressure values (at 1 MHz frequency) that will cause US-induced lung haemorrhage in selected adult mammals and human, according to the membrane models of alveolar wall facet	96
Table A1	The minimum bending stiffness of alveolar wall facet in selected adult mammals and human	129
Table A2	The minimum values of $Q_{medium}$ of the alveolar wall facet at 1 MHz frequency for selected adult mammals and human	131
Table A3	Alveolar dimensions for selected adult mammals and human	135
Table A4	Basic arithmetic operations for intervals and ranges	136
Table A5	The threshold pressures of the membrane models of alveolar resonance mechanism and of the experimental past studies on US-induced lung haemorrhage. The experimental data are obtained from the compilation by Church CC & O'Brien Jr WD (2007) and also from Tarantal AF & Canfield DR (1994) while theoretical data are generated by this study	137
Table A6	The typical US frequency used in US imaging of human structures and its penetration depth	141

## LIST OF FIGURES

		Pg.
Figure 2.1	The macroscopic and microscopic images of the US-induced lung haemorrhage in adult rats (Zachery JF et al., 2006).	10
Figure 2.2	The alveolus as the pulmonary gas exchanger.	16
Figure 2.3	(a) The alveolus represented as a dodecahedron (MacLean KJM, 2007). (b) The arrangement pattern of alveoli akin to froth or honeycomb (SRJC, 2013).	18
Figure 2.4	The BGB within an alveolar wall (West JB & Mathieu-Costello O, 1992).	19
Figure 2.5	The incident longitudinal wave being reflected and refracted as longitudinal and transverse waves at the interface of media.	24
Figure 2.6	Flow of the basic modelling process.	25
Figure 2.7	The plane axes ( $x, y$ ) and forces ( $T\partial x, T\partial y$ ) on a membrane element ( $\partial y-\partial x$ ) with transverse displacement axis, $z$ .	29
Figure 2.8	Longitudinal wave impinging normally and exciting a membrane.	31
Figure 2.9	A spring-mass-damper system depicting the equivalent SDOF vibration.	32
Figure 2.10	The vector diagrams for the eqn.2.23.	34
Figure 3.1	Flow of the modelling and vibration analysis process for the theoretical study of alveolar resonance mechanism.	38
Figure 3.2	(a) Square membrane model, (b) Circular membrane model; representing the pentagonal alveolar wall facet.	41
Figure 3.3	The Cartesian coordinate system describes the boundaries of the square membrane model.	42
Figure 3.4	The various vibration patterns of the square membrane model at few initial resonant modes; (a) $n_x, n_y = 1, 1$ ; (b) $n_x, n_y = 1, 2$ and (c) $n_x, n_y = 2, 1$ (Saad MH, 2009).	44
Figure 3.5	The polar coordinate system describes the boundary of the circular membrane model (Corrigan A, 2001).	45
Figure 3.6	The Bessel functions of the first kind for 0 <sup>th</sup> – 5 <sup>th</sup> order (DPlot, 2013).	49

Figure 3.7	Various vibration patterns of the circular membrane model at few initial resonant modes; (a) $n = 1$ , (b) $n = 2$ and (c) $n = 3$ (Woodhouse J, 2011).	50
Figure 3.8	The square membrane model of alveolar wall facet at rest.	57
Figure 3.9	(a) The deformation of square membrane model at fundamental mode (Petitgrand S et al., 2001). (b) Square-based pyramid as an approximation.	58
Figure 3.10	The circular membrane model of alveolar wall facet at rest.	59
Figure 3.11	(a) Deformation of circular membrane model at fundamental mode (Woodhouse J, 2011). (b) The spherical cap as an approximation.	59
Figure 3.12	The approximation of the length dimensions of the membrane models of the alveolar wall facet.	64
Figure 4.1	Relationship between the range of transverse wave velocity and the varying areal strain of tidal breath (0 – 0.1025) in membranes models of the alveolar wall facet.	68
Figure 4.2	The range of fundamental frequency vs. areal strain of tidal breath (0 – 0.1025) of the: (a) square membrane model (b) circular membrane model, for the adult mouse and rat.	71
Figure 4.3	The range of fundamental frequency vs. areal strain of tidal breath (0 – 0.1025) of the: (a) square membrane model (b) circular membrane model, for the adult rabbit and dog.	72
Figure 4.4	The range of fundamental frequency vs. areal strain of tidal breath (0 – 0.1025) of the: (a) square membrane model (b) circular membrane model, for the adult pig.	73
Figure 4.5	The range of fundamental frequency vs. areal strain of tidal breath (0 – 0.1025) of the: (a) square membrane model (b) circular membrane model, for the adult cat and monkey.	74
Figure 4.6	The range of fundamental frequency vs. areal strain of tidal breath (0 – 0.1025) of the: (a) square membrane model (b) circular membrane model, for the adult human.	75
Figure 4.7	The value of resonant frequencies of the: (a) square membrane model, (b) circular membrane model; for adult human with mean alveolar length dimension at transverse wave velocity of 100 m/s.	78

Figure 4.8	The vibration amplitude vs. frequency at various Q-factor values for the square membrane model of alveolar wall facet for adult human. The fundamental frequency is set at 1.729 MHz while the peak pressure of driving US waves is 1 MPa.	82
Figure 4.9	The vibration amplitude vs. frequency at various Q-factor values for the circular membrane model of alveolar wall facet for adult human. The fundamental frequency is set at 1.834 MHz while the peak pressure of driving US waves is 1 MPa.	83
Figure 4.10	The deflection of membrane models at fundamental mode resonance.	85
Figure 4.11	Deflection angle vs. areal strain of resonance for: (a) square membrane model, (b) circular membrane model, of alveolar wall facet at fundamental mode.	87
Figure 4.12	The theoretical curves of threshold pressure vs. fundamental frequency of alveolar resonance mechanism for adult mouse, together with the plotted past experimental data of US-induced lung haemorrhage in the adult mouse. An experimental data (2.8, 3.6) is an outlier and is omitted from chi-square calculation.	91
Figure 4.13	The theoretical curves of threshold pressure vs. fundamental frequency of alveolar resonance mechanism for adult rat, together with the plotted past experimental data of US-induced lung haemorrhage in the adult rat.	91
Figure 4.14	The theoretical curves of threshold pressure vs. fundamental frequency of alveolar resonance mechanism for adult rabbit, together with the plotted past experimental data of US-induced lung haemorrhage in the adult rabbit. This experimental data is however outside the curves' range.	92
Figure 4.15	The theoretical curves of threshold pressure vs. fundamental frequency of alveolar resonance mechanism for adult dog. There are no past experimental data of US-induced lung haemorrhage in adult dog to be plotted.	92
Figure 4.16	The theoretical curves of threshold pressure vs. fundamental frequency of alveolar resonance mechanism for adult pig, together with the plotted past experimental data of US-induced lung haemorrhage in the neonatal pig. Only neonatal pig data are available and plotted.	93
Figure 4.17	The theoretical curves of threshold pressure vs. fundamental frequency of alveolar resonance mechanism for adult cat. There are no past experimental data of US-induced lung haemorrhage in the adult cat to be plotted.	93

Figure 4.18	The theoretical curves of threshold pressure vs. fundamental frequency of alveolar resonance mechanism for adult monkey, together with the plotted past experimental data of US-induced lung haemorrhage in the adult monkey. This experimental data value is however outside the curves' range.	94
Figure 4.19	The theoretical curves of threshold pressure vs. fundamental frequency of alveolar resonance mechanism for adult human, together with the plotted MI = 1.9 limit line. There are no past experimental data of US-induced lung haemorrhage in the adult human to be plotted.	94
Figure A1	Forces on an arbitrary element of membrane (SEU, 2012).	126
Figure A2	The deformation of area in a membrane.	130
Figure A3	Range graph with upper and lower limits.	136

## LIST OF SYMBOLS

$\alpha, \beta$	deflection angles
$\gamma$	damping factor
$\varepsilon$	areal strain
$\varepsilon_b$	areal strain of tidal breath
$\varepsilon_r$	areal strain of resonance
$\varepsilon_y$	yield areal strain
$\eta$	linear strain
$\kappa$	polytropic index of gas
$\tilde{\lambda}$	wavelength
$\lambda$	stretch ratio
$\rho$	density
$\sigma$	area density
$\sigma_{eq}$	equivalent area density
$\chi^2$	chi-square goodness of fit
$\psi$	surface tension coefficient
$\omega_o$	fundamental angular frequency
$\phi$	phase angle
$\theta$	azimuthal angle
$\Omega$	acoustic impedance of air
$a$	acceleration
$A$	area
$A_0$	initial area
$A_1$	final area
$b_{eq}$	equivalent damping constant
$B$	AVMI factor
$c_L$	longitudinal wave speed
$c_T$	transverse wave velocity
CO <sub>2</sub>	carbon dioxide
$d$	thickness
$D_e$	bending stiffness
$E$	Young's modulus

$f$	linear frequency
$f_m$	frequency in medium
$f_n$	resonant frequency of circular membrane
$f_{n_x, n_y}$	resonant frequency of square membrane
$f_v$	frequency in vacuum
$f_l$	fundamental frequency of circular membrane
$f_{l, l}$	fundamental frequency of square membrane
$F$	force
$F_D$	driving force
$F_E$	elastic force
$F_o$	peak amplitude force
$F_R$	resistive force of the damping
$G$	shear modulus
$J$	support-loss coefficient
$J_0(h)$	Bessel function of the first kind for 0 <sup>th</sup> order
$k$	wave number
$K$	bulk modulus
$k_{stretch}$	constant of proportionality in stretching
$L$	side-length
$L_0$	initial length
$L_1$	final length
$L_i$	incident longitudinal wave
$L_r$	reflected longitudinal wave
$L_t$	refracted longitudinal wave
$m$	mass
$m_{eq}$	equivalent mass
$MI$	mechanical index
$n$	mode of circular membrane
$n_x, n_y$	mode of square membrane
$N$	normal force
$O_2$	oxygen
$O_i$	observed empirical data
$p$	number of sets of data

$P$	pressure
$P_o$	threshold pressure
$P_{r.3}$	derated peak rarefactional pressure
$Q$	quality factor
$Q_{medium}$	quality factor of medium damping
$Q_{support}$	quality factor of membrane's support loss
$Q_{surface}$	quality factor of membrane's surface loss
$Q_{TED}$	quality factor of thermal-elastic damping
$r$	distance from origin
$r_o$	radius
$S_i$	expected theoretical data
$s_{eq}$	equivalent spring constant
$t$	time
$T$	tension
$Tr$	reflected transverse wave
$Tt$	refracted transverse wave
$u$	Poisson's ratio
$U_e$	stretching energy
$v$	velocity
$\nabla^2$	Laplacian Operator
$w$	angular frequency of waves
$x$	x-axis
$y$	y-axis
$z$	z-axis / transverse displacement
$Z$	amplitude
$Z_{max}$	maximum amplitude at resonance

## LIST OF ABBREVIATIONS

AIUM	American Institute of Ultrasound in Medicine
ALARA	as low as reasonably achievable
AVMI	added virtual mass increment
BGB	blood-gas barrier
BMUS	British Medical Ultrasound Society
ECM	extra-cellular matrix
ECMUS	European Committee for Medical Ultrasound Safety
ED <sub>05</sub>	effective dose for 5% incident risk of US-induced lung haemorrhage
eqn.	equation
FDA	Food & Drug Administration
ISPPA <sub>3</sub>	derated spatial peak pulse average intensity
MDOF	multiple degree-of-freedom
MI	mechanical index
NCRP	National Council on Radiation Protection and Measurements
NEMA	National Electrical Manufacturers Association
Q-factor	quality factor
RV	residual volume
SEU	Southeast University
SDOF	single degree-of-freedom
SRJC	Santa Rosa Junior College
TI	thermal index
TLC	total lung capacity
US	ultrasound
WFUMB	World Federation for Ultrasound in Medicine and Biology

**PERMODELAN DAN ANALISIS GETARAN UNTUK  
MEKANISMA RESONANS ALVEOLUS BAGI  
PENDARAHAN PARU-PARU AKIBAT ULTRASOUND**

**ABSTRAK**

Kesan buruk biologi diagnostik ultrasound yang dikaji secara meluas adalah pendarahan paru-paru akibat ultrasound. Pendarahan paru-paru akibat ultrasound telah banyak di laporkan berlaku dalam experimentasi menggunakan pelbagai haiwan. Namun begitu, mekanisma yang menyebabkan pendarahan paru-paru akibat ultrasound masih belum dikenalpasti. Salah satu daripada mekanisma pendarahan paru-paru akibat ultrasound yang dicadangkan tapi belum dikaji adalah mekanisma resonans alveolus. Mekanisma resonans alveolus dihipotesiskan sebagai getaran paksa struktur alveolus oleh gelombang ultrasound luaran. Kajian permodelan dan analisis getaran ini, menyiasat secara teori mekanisma resonans alveolus dan keupayaannya untuk menyebabkan pendarahan paru-paru akibat ultrasound. Pertama sekali, segi-segi dinding alveolus telah dimodelkan sebagai membran berbentuk segiempat-sama dan bulatan bersempadan tetap. Aplikasi teori getaran linear bersama hukum-hukum kekenyalan linear ke atas model-model membran ini, seterusnya menghasilkan persamaan-persamaan frekuensi asas dan tekanan ambang. Frekuensi asas model membran mewakili frekuensi asli struktur alveolus, yang di mana resonans boleh berlaku. Manakala, tekanan ambang adalah tekanan minimum ultrasound untuk mengakibatkan kerosakan dan mencetuskan pendarahan di dinding alveolus. Seterusnya, data teori telah digenerasi dengan mengaplikasikan persamaan-persamaan frekuensi asas dan tekanan ambang setiap model membran ke atas mamalia dewasa terpilih dan manusia. Data teori menunjukkan bahawa

frekuensi asli struktur alveolus berada dalam lingkungan frekuensi megahertz diagnostik ultrasound. Maka gelombang ultrasound diagnostik mampu menyebabkan resonans ke atas alveolus. Data teori ini juga telah dibandingkan dengan data experimen pendarahan paru-paru akibat ultrasound dari kajian-kajian lepas yang dilakukan ke atas haiwan untuk tujuan validasi. Kajian ini mendapati bahawa penggunaan model-model membran mekanisma getaran alveolus bagi mengkaji pendarahan paru-paru akibat ultrasound, divalidasikan dengan kebarangkalian 95%. Oleh kerana itu, mekanisma resonans alveolus boleh dianggap sebagai mekanisma mungkin penyebab pendarahan paru-paru akibat ultrasound dan model-model membran mewakilinya dengan baik. Seterusnya kajian ini meramalkan bahawa pendarahan paru-paru akibat ultrasound boleh dielakkan jika pernafasan adalah  $\leq 20\%$  daripada kapasiti penuh paru-paru, TLC (untuk semua mamalia dewasa dan manusia) dan jika frekuensi ultrasound dikekalkan  $> 1.69$  MHz bila indeks mekanikal, MI adalah  $\leq 1.9$  (untuk manusia dewasa).

**MODELLING AND VIBRATION ANALYSIS OF  
ALVEOLAR RESONANCE MECHANISM OF  
ULTRASOUND-INDUCED  
LUNG HAEMORRHAGE**

**ABSTRACT**

The most widely studied biological adverse effect of the diagnostic ultrasound is the ultrasound-induced lung haemorrhage. The ultrasound-induced lung haemorrhage has been observed in various experimental studies on animals. Nevertheless, the actual mechanism by which the ultrasound-induced lung haemorrhage occurs still remains undetermined and unproven. One of the proposed but unexplored mechanisms is the alveolar resonance mechanism. The hypothetical alveolar resonance mechanism is proposed as the forced vibration and resonance of the alveolar structure by the external ultrasound waves. This modelling and vibration analysis study, theoretically investigates the alveolar resonance mechanism and its capability for producing the ultrasound-induced lung haemorrhage. Firstly, the facet of the alveolar wall was modelled as square and circular membranes with fixed-boundary. Then, the application of the linear theory of vibration together with the laws of linear elasticity, unto the membrane models, produced the equations of fundamental frequency and threshold pressure. The fundamental frequency of each membrane model represents the natural frequency of the alveolar structure at which the alveolar resonance mechanism may occur. Meanwhile, the threshold pressure of each membrane model determines the minimum pressure of ultrasound needed to cause alveolar structural failure, resulting in the ultrasound-induced lung haemorrhage. Next, theoretical data were generated by applying the equations of

fundamental frequency and threshold pressure of this study to selected adult mammals and human. The theoretical data show that the fundamental frequency of the alveolar wall facet to be within the megahertz frequency range of diagnostic ultrasound. Thus, alveolar structure can be resonated by the diagnostic ultrasound waves. The theoretical data were further compared against past experimental data of ultrasound-induced lung haemorrhage in animals, for validation purpose. It is found that this modelling and vibration analysis of the alveolar resonance mechanism is validated at 95% confidence level, for studying the ultrasound-induced lung haemorrhage. Therefore, the alveolar resonance mechanism can be duly considered as a plausible mechanism of the ultrasound-induced lung haemorrhage and the membrane models of alveolar wall facet of this study adequately describe it. This study consequently predicts that the ultrasound-induced lung haemorrhage can be deterred if the tidal breath is  $\leq 20\%$  of the total lung capacity, TLC (for adult mammals and human) and if the frequency of ultrasound is kept  $> 1.69$  MHz while the mechanical index, MI is  $\leq 1.9$  (for adult human).

# CHAPTER 1

## INTRODUCTION

### 1.1 Research Background

The diagnostic ultrasound (US) imaging is widely utilized in the medical institution as a safe and useful imaging technique. It is often used to obtain images of soft tissues and also of the foetus. From the obtained images; diagnosis concerning tissue structures, internal liquid flow and the progress of pregnancy is possible. The diagnostic US imaging normally employs frequency in the megahertz range and pressure in the megapascal range. Higher frequency produces higher resolution in images but with a reduction in penetration depth, and vice-versa. The mechanical index (MI) is determined from the pressure and the frequency of the US. According to the regulations of the Food & Drug Administration (FDA) of the United States of America, the MI for diagnostic US imaging should be  $\leq 1.9$ . Other parameters normally present and often considered in US exposure are the pulse duration, pulse repetition frequency and the exposure duration.

Contrary to the public perception and understanding, the US does have biological side-effects even at diagnostic exposure levels. The diagnostic US has been reported to cause damage to cells, tissues and organs. Therefore just alike most other medical imaging techniques, the diagnostic US imaging should be used according to its safety protocols as it can be detrimental to health.

One of the most widely studied sites of bioeffect induced by US is the lungs. The US-induced lung haemorrhage or bleeding has been experimentally observed many

times in laboratory animals at the exposure levels of diagnostic US. The bleeding in the lungs occurs only during the US exposure and originates from within the alveolar wall. The US-induced lung haemorrhage however has not been observed or proven to occur in human. This fact is due to the existence of several limitations for conducting US exposure studies on human. These limitations are; the unfeasibility of epidemiological study on human population, the non-standardized recording of clinical US exposures and the legality and moral question of detrimental experimentations on living human.

Several mechanisms have been proposed in order to explain the phenomenon of the US-induced lung haemorrhage. These mechanisms are classed down by the two ways the US can interact and damage the tissues within the body, which are thermally and mechanically. In thermal mechanism, the US energy is basically converted into heat energy and the temperature of the tissues is increased. A significant increase in temperature affects tissues by modifying or damaging the protein structures. The thermal mechanism may occur at the interface of soft tissues and bone or air. The difference in acoustic impedance between mediums promotes the conversion of US mechanical energy into heat energy. The thermal mechanism; however, was proven conclusively as not the cause of the US-induced lung haemorrhage.

In mechanical mechanism, damages to tissues are inflicted when the incident US waves cause unnatural motion of tissue structure or other elements within. For example, the mechanical mechanism known as inertial cavitations produces violent collapse of micro-bubbles that exist within certain tissue structures. These micro-bubbles undergo forced vibration by the US waves. They oscillate and grow and

burst at certain conditions, resulting in the sudden release of energy that can destroy surrounding tissues. The inertial cavitations mechanism is thought to occur mainly in air-rich tissue structures. However, the introduction of the gas-filled micro-contrast agent into the body during some US imaging procedure (of soft tissues structure), may allow the inertial cavitations mechanism to occur in other parts of the body too. As the lung is a structure continuously filled with air, the mechanical mechanism that causes US-induced lung haemorrhage was naturally thought to be the inertial cavitations of micro-bubbles. Nevertheless, the inertial cavitations mechanism was subsequently proven as not the cause of the US-induced lung haemorrhage.

There is another mechanical mechanism known as the alveolar resonance that has been tentatively proposed as the cause of the US-induced lung haemorrhage. This mechanical mechanism is hypothetical as it yet to be explored theoretically or experimentally. In the alveolar resonance mechanism, the alveolar structure of lungs under US exposure is described as being ably vibrated into resonance. Excessive vibration during resonance may then damage the tissues or cells within. However, it is said that the alveolar size is too large for the alveolus to resonate, alike the micro-bubbles. Thus, the proposed alveolar resonance mechanism is not treated seriously and has not been a focus in the study of the US-induced lung haemorrhage.

## **1.2 Research Problems**

There are some unresolved problems in the field of US-induced lung haemorrhage. Until now, the actual mechanism through which the US-induced lung haemorrhage occurs, still has not been determined or proven conclusively in any way. Past

researches had focused almost solely on the inertial cavitations mechanism and ignored other viable mechanical mechanisms. Another obvious dilemma is that the US-induced lung haemorrhage occurs readily in laboratory animals, but in human it is not known to occur and is yet to be extensively studied. Finally, the precautionary measures to be taken to avoid possible occurrence of US-induced lung haemorrhage, during clinical diagnostic US imaging of human, have not been identified yet.

### **1.3 Objectives of Study**

This theoretical study focuses on the hypothetical alveolar resonance mechanism and its possible role in the US-induced lung haemorrhage. The objectives of this study are:

- i. To develop vibration model(s) of the alveolar resonance mechanism in order to determine the resonant frequency and the threshold pressure needed to cause the US-induced lung haemorrhage.
- ii. To apply and analyze the developed vibration model(s) of the alveolar resonance mechanism in various mammals and human, in order to generate theoretical data for verifications and validation purposes.
- iii. To utilize the developed vibration model(s) of the alveolar resonance mechanism in discussing the past experimental results of the US-induced lung haemorrhage and in obtaining predictions and precautionary recommendations.

#### **1.4 Scope of Research**

This study explores only the theoretical aspect of the hypothetical alveolar resonance mechanism and its capability in causing the US-induced lung haemorrhage. The alveolar structure is modelled and subjected to vibration analysis, using the linear theory of vibration and laws of linear elasticity. The developed models and derived equations are then applied to selected adult mammals and human to generate theoretical data. The theoretical data are used for verification, validation and predictions concerning the US-induced lung haemorrhage.

#### **1.5 Outline of Thesis**

This thesis is broadly arranged into chapters. This is Chapter One and it gives the research background, problems and scope. The objectives of this theoretical study are expounded and the outline of thesis is described too. The Chapter Two introduces the topic of the US-induced lung haemorrhage. The mechanisms of inertial cavitations and alveolar resonance are briefly discussed here. The alveolus structure; its behaviour, alveolar wall and strains are also studied. The US characteristics and wave propagation modes are described. An introduction to modelling and vibration analysis is further given. Certain aspects of the linear vibration theory and the theory of linear elasticity are also analyzed.

In Chapter Three, the process of modelling and vibration analysis of this theoretical study on alveolar resonance mechanism is discussed. Justifiable assumptions are presented and the alveolar structure is simplified and modelled. Then; the resonant

frequencies, forced vibration, resonant amplitudes and the strains involved are analyzed too. Their equations are obtained through the applications of the linear theory of vibration and also the laws of linear elasticity. The threshold pressure equations for alveolar structural damage are subsequently derived. Furthermore various adult mammals and human are selected for this study and their alveolar dimensions are determined from available literatures.

Chapter Four contains calculations, generated data and discussion based on the equations obtained and derived in the previous chapter. Firstly, the equations are applied to selected adult mammals and human to generate theoretical data. The derived equations are examined and verified along the way. Later, the theoretical data are compared to the past experimental data regarding US-induced lung haemorrhage, for validation purposes. Further predictions and precautions concerning the US-induced lung haemorrhage are then determined based on the results of this study. Finally, the justification of the method of modelling is given while the limitations of this study are analyzed. This thesis closes with the Chapter Five which summarizes the results and answers the objectives of this theoretical study on alveolar resonance mechanism.

## **CHAPTER 2**

### **LITERATURE REVIEW AND THEORY**

In the section on literature review, the bioeffects of US and the US-induced lung haemorrhage are initially introduced. The inertial cavitations mechanism and the hypothetical alveolar resonance mechanism are also briefly described. Later; the alveolar structure and its characteristics, its components and strains are studied too. The risk indicators for US bioeffects are also discussed. In the section on theory, the US characteristics and wave propagation modes are analyzed. Furthermore, the modelling technique and vibration analysis method are also explored. Finally, the physical theories applicable for this study concerning the two-dimensional wave equation, forced vibration and strains are introduced.

#### **2.1 Literature Review**

##### **2.1.1 The Bioeffects of Ultrasound**

The US in general was thought to be relatively safe until the year 1951, when researchers involved with the development of US equipments became aware of the harmful effects of high intensity US on tissues and organs (French LA et al., 1951). Initial investigations concerning the damages induced by high intensity US on the nerve tissues was done by Fry WJ (1953); while on the eye and ocular adnexa by Baum G (1956). Insomuch, the ability of the high intensity US in inducing damages were proposed as early dose measurements. Purnell EW et al. (1964); proposed that the duration of US exposure for producing observable cataract of the eye to be known as cataract producing unit. Meanwhile, a damage ability index was used to

describe the spinal cord damage induced by US (Taylor KJW & Pond JB, 1972). All these early US bioeffects were; however, observed and obtained at very high values of US intensity of 50 – 1500 W/cm<sup>2</sup> (Hueter TF et al., 1956).

The US is widely applied nowadays in the medical field, as a useful tool for non-invasive diagnostic imaging and therapy. The approved intensity used in the diagnostic US imaging is from 7 mW/cm<sup>2</sup> (for eye) to 100 mW/cm<sup>2</sup> (for other organs), while for the US therapy is ~3 W/cm<sup>2</sup> (Rossing TD, 2007). The frequency of the US normally used for diagnostic imaging purposes is in the range of 1 – 10 MHz, depending on the procedures (Dalecki D, 2004). Intracranial imaging, musculoskeletal imaging, exploratory imaging and sometimes deep organs imaging (in obese patients); utilize low US frequencies of ~1 MHz (Barnes RW & Riley WA, 1980 and Markowitz J, 2011). Low level frequencies give deeper penetration but at the cost of low spatial resolution. Medium level frequencies (2.5 – 5.0 MHz) are used in normal thoracic, abdominal, and pelvic and obstetrics examinations (Fitzgibbons RJ & Greenburg AG, 2001). Meanwhile, high level frequencies (5.0 – 10.0 MHz) are used to obtain high spatial resolution images of superficial structure such as breasts, testes and thyroid (Brant WE & Helms CA, 2006). Abnormally very high frequencies of 15.0 MHz and 20.0 MHz are respectively utilized in imaging the subcutaneous structure and skin. A recent use of diagnostic US is for pneumothorax detection and it employs frequencies of 2.0 – 10.0 MHz (Noble VE, 2012).

Nevertheless, *in vitro* tissue study and *in vivo* animal experimentations show that the US at diagnostic intensity and frequency levels can cause variety of bioeffects (Dalecki D, 2004). Exposures to diagnostic US have been observed to produce lung

haemorrhage and intestinal haemorrhage in animals (Child SZ et al., 1990 and Dalecki D et al., 1995). Sensory organs located near bones such as ears and eyes are susceptible to detrimental thermal effects caused by US. Cell fibroblast and cell lysis due to diagnostic US have also been reported (Ward M et al, 1999). Therefore, the concerns and safety regarding the clinical use of diagnostic US imaging on human are continuously raised and addressed for years by the ultrasound research communities such as the World Federation for Ultrasound in Medicine and Biology (WFUMB, 1996), American Institute of Ultrasound in Medicine (AIUM, 2000b) and British Medical Ultrasound Society (BMUS, 2010). When compared to other medical imaging procedures, the clinical use of the diagnostic US imaging on humans has had remarkable safety record with no documented cases of adverse effects (NCRP, 2002). Actually, the diagnostic US imaging of humans is assumed as a safe procedure in the absence of plausible and confirmed clinical evidences. The question of whether the US-induced bioeffects can happen in human during diagnostic US imaging and its implications, are yet to be studied and answered.

### **2.1.2 The Ultrasound-Induced Lung Haemorrhage**

The downside of diagnostic US imaging is that it is laboratory proven to cause bioeffects on the tissues and organs of animals. Particularly in the lungs, the US interactions and its resulting bioeffect are seen to be intensified because the lungs are such delicate structure with many thin air-tissue interfaces (Church CC & O'Brien Jr WD, 2007). The large difference of acoustic impedance between tissue and air promotes energy absorption within the lungs and hence the intensity of the damage. The foetal lungs are; however, not affected by US (Hartman C et al, 1990) as they are constantly filled with amniotic fluid (Stratmeyer ME et al, 2008). The interface in

foetal lungs is liquid-tissue (small difference of acoustic impedance) instead of air-tissue, prompting high transmittance of US waves and low energy absorption in the lungs.

The US-induced lung haemorrhage has been observed in animal experimentations at the exposure levels of the diagnostic US imaging. The first reported experimental US-induced lung haemorrhage is in adult mice at exposure values; pressure threshold = 1 MPa, frequency = 2 MHz, pulse duration = 10  $\mu$ s, pulse repetition frequency = 100 Hz and exposure duration = 3 min (Child SZ et al., 1990). Since then, the US-induced lung haemorrhage has been observed in other animals such as rats, rabbits, apes and pigs at similar exposure conditions (Zachery JF & O'Brien Jr WD, 1995; Tarantal AF & Canfield DR, 1994; Baggs R et al., 1996; Dalecki D et al., 1997b and Zachery JF et al., 2001). The Figure 2.1 shows macroscopically and microscopically, the US-induced lung haemorrhage.

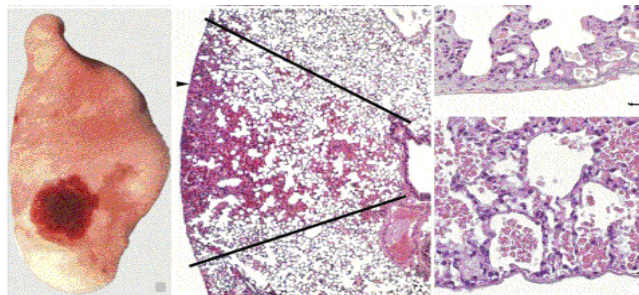


Figure 2.1: The macroscopic and microscopic images of the US-induced lung haemorrhage in adult rats (Zachery JF et al., 2006).

The lung haemorrhage induced by US, originates from within the alveolar wall at the level of the blood-gas barrier (BGB) (AIUM, 2000b). It is characterized by the localized extravasations of red blood cells from the pulmonary capillaries into the alveolar spaces (Penney DP et al., 1993). Hence, the lung haemorrhage is due to

damaged microvasculature and not to damaged arterioles, venules, bronchioles or distal airways of the lung. ECMUS (1999), states that the rupturing of the pulmonary capillaries and the alveolar epithelium and endothelium in the BGB, is the reason for the US-induced lung haemorrhage. Ruptures in BGB can occur when the BGB is relatively displaced (Howard D & Sturtevant B, 1997). Furthermore, the damage that causes lung haemorrhage is non-progressive, in other words, only seen to occur during US exposure (Zachery JF et al., 2001). This damage can be repaired with time by the intercellular lipid stores within the alveolar walls (Vlahakis NE & Hubmayr RD, 2000), but scarring and fibrosis can still result.

In the usage of diagnostic US on humans, the lungs are only ultrasonically scanned for the detection of fluid within (pneumothorax) (Noble VE, 2012). Hence, the lungs are directly exposed to US only in this procedure. Other than that, the US imaging is not applicable for the lungs as the air within cause artefacts. Nevertheless, other US imaging procedures on the human abdominal and thoracic regions may expose the lungs to indirect and accidental US waves. The duration of these indirect and accidental exposures are estimated at 10 seconds per procedure (O' Brien Jr WD et al., 2006). In animal experimentations, lungs haemorrhage has been observed within this short exposure duration of US. Presently, there is no evidence of the US-induced lung haemorrhage occurring or not occurring in human. This is largely due to the lack of experimental studies on humans. Only a single study reports that the US-induced lung haemorrhage is not observed in humans at a minimum frequency of 3.5 MHz while maximum pressure is 2.4 MPa (Meltzer RS et al., 1998). Therefore the question of scaling persists, of whether the effects seen in animals can be extrapolated to effects in humans (ter Haar GR, 2010). AIUM (2000b) also ponders

on the possible conditions for the US-induced lung haemorrhage becoming significant in humans, and the resulting clinical and physiological implications. The US-induced lung haemorrhage; however, might not occur in human because of the differences in lung composition and dimensions (AIUM, 2000b).

Both thermal and mechanical mechanisms have been proposed as to explain and understand how the US-induced lung haemorrhage occurs. The thermal mechanism is the heating effect by the US waves (Barnett SB, 2000). A slight increase in temperature can alter the functionality of enzymes, coagulate protein and kill cells (O'Brien Jr WD et al., 2000). Nevertheless, the thermal mechanism has been experimentally ruled out from being the mechanism of US-induced lung haemorrhage by Hartman CL et al. (1992); using thermocouple measurements, and also by Zachery JF et al. (2006); using pathological analysis of laser-induced lesion.

Certain mechanical mechanism is thus believed to cause the US-induced lung haemorrhage. Mechanical mechanisms are phenomena that produce motion with negligible temperature change of  $< 1^{\circ}\text{C}$  (Stratmeyer et al., 2008). A few mechanical mechanisms are proposed and considered for the US-induced lung haemorrhage. They are the inertial cavitations mechanism, involving the bursting of micro-bubbles which might damage surrounding tissues; the alveolar resonance mechanism, that produce vibration and strain in alveolar structure leading to membrane wounding; and the interface boundary mechanism, where acoustic impedance difference cause sudden energy release and rupturing of interface (ECMUS, 1999). The exact and actual mechanical mechanism responsible for the US-induced lung haemorrhage is yet to be conclusively determined or proven (AIUM, 2000b).

### 2.1.3 Inertial Cavitations Mechanism

The mechanical mechanism known as the inertial cavitations has been widely researched in the study of US-induced lung haemorrhage. At the exposure levels of diagnostic US, this mechanism requires the presence of gas in tissue structures (lungs and intestines) or an injection of gas-filled contrast agent (Rott HD, 1997 and O'Brien Jr WD et al., 2004). The existence of air-tissue interfaces in the alveoli renders the lungs vulnerable to the possible formation and presence of micro-bubbles. Inertial cavitations mechanism is the rapid growth and bursting of micro-bubbles through resonance induced by US waves. The bursting micro-bubbles produce high energy emanations and micro-jets that can damage surrounding tissues (Kudo N & Yamamoto K, 2004). If the micro-bubbles just resonate without bursting, then it is just known as transient cavitations. The maximum response of cavitations occurs at the resonant frequencies of micro-bubbles, which depend on the initial size of micro-bubbles. The fundamental frequency of micro-bubbles in unbounded medium follows the Rayleigh-Plesset equation as (Qin S & Ferrara KW, 2007)

$$f_1 = \frac{1}{2\pi} \sqrt{\frac{3\kappa(P_i + 2\psi / r_i)}{\rho_m r_i^2} - \frac{2\psi}{\rho_m r_i^3}} \quad (2.1)$$

where the polytropic index of gas,  $\kappa = 1.0$ ; the initial pressure in medium,  $P_i = 101325$  Pa; density of medium (blood),  $\rho_m = 1090$  kg/m<sup>3</sup>; surface tension coefficient,  $\psi = 0.0643$  N/m and the initial radius of micro-bubble is  $r_i$ .

The size of micro-bubbles should be a few microns in radius in order to resonate and to be affected by the frequency range of diagnostic US imaging (Dalecki D, 2004). The threshold for the inertial cavitations of micro-bubbles and gas-filled contrast

agent depends primarily on the US pressure and frequency (ECMUS, 1999). Inertial cavitations of the micro-bubbles approximately occur at  $MI = 0.7$  while for the gas-filled contrast agent at  $MI = 0.3$  (Dendy PP & Heaton B, 2011).

A review by Carstensen EL et al. (2000) first raised doubts regarding the inertial cavitations as being the mechanism of US-induced lung haemorrhage. The findings of several experimental studies on US-induced lung haemorrhage are inconsistent with the theory of inertial cavitations mechanism. Inertial cavitations mechanism basically requires the presence of micro-bubbles. Although alveoli contain air, it is reported to be in diffused form and there is no evidence of micro-bubbles existing in the alveoli (Frizzel LA et al., 2001). It is further shown that the introduction of gas-filled contrast agent do not increase of the extent of lung haemorrhage when it should (Raeman CH et al., 1997 and O'Brien Jr WD et al., 2004). In theory, the occurrence threshold of inertial cavitations should be lowered as the threshold MI for the gas-filled contrast agent is lower than for micro-bubbles (ECMUS, 1999).

In theory, the inertial cavitations mechanism depends solely on the peak negative pressure and not the peak positive pressure of the US, as it regards the micro-bubbles to be constrained by surrounding medium (Bailey MR et al., 1996). Increased hydrostatic pressure reduces the peak negative pressure and hence inertial cavitations. Nevertheless, according to a lung overpressure study by Frizzell LA et al. (2003), the occurrence of US-induced lung haemorrhage does not correlate with the US peak negative pressure. In fact, O'Brien Jr WD et al. (2000) finds that lung overpressure enhanced the US-induced lung haemorrhage. All these prove that the inertial cavitations mechanism is not the cause of the US-induced lung haemorrhage.

#### **2.1.4 Alveolar Resonance Mechanism**

Another mechanical mechanism suggested in order to explain the US-induced lung haemorrhage, is the alveolar resonance mechanism. This mechanism is hypothetical and has not been experimentally tested or theoretically developed yet. The alveolar resonance mechanism is proposed as the oscillatory response of the alveolus to the US compression and tensional waves (Church CC et al., 2008). The alveolar structure thus deforms rhythmically from its equilibrium state. Consequently, this produces detrimental strain on a tissue structure not meant to move in such fashion (Nyborg WL, 1982). The deformation can also produce local stresses on neighbouring and surrounding tissues (Vivino AA et al., 1985 and Everbach EC et al., 1999). ECMUS (1999), states that the US at diagnostic frequency levels might cause alveolar resonance which may then lead to disruption of the alveolar capillaries and membranes, resulting in haemorrhaging.

There are two primary conditions for alveolar resonance to occur and to be able to produce damage in the lungs. A primary condition is the resonant frequency of the alveolar structure. The resonant frequency of the alveolar structure must be within the megahertz range of diagnostic US frequency for resonance to occur. According to the Rayleigh-Plesset equation (eqn.2.1), the whole alveolus is too large to oscillate in response to the US waves (O'Brien Jr WD et al., 2000). Nevertheless, ter Haar GR (2010) states that the forced vibration and resonance of large gas bodies such as the alveoli is probably different than the inertial cavitations of micro-bubbles. Thus, the equation of resonant frequency for the alveolar structure should be derived directly from the theory developed specifically for the alveolar resonance mechanism.

The other primary condition is the threshold pressure for causing structural damage of the alveolus. This threshold pressure should be within the megapascal range of diagnostic US pressure for the US-induced lung haemorrhage to occur. The threshold pressure equation of alveolar resonance mechanism for causing the US-induced lung haemorrhage has not been derived yet in literature.

No theoretical or experimental studies have been conducted concerning the hypothetical alveolar resonance mechanism and its probable role in producing the US-induced lung haemorrhage (ECMUS, 1999). A thorough survey of literature gave no indication that the hypothetical alveolar resonance mechanism has been explored in any way. Most of the past researches have had focused on the inertial cavitations mechanism which is now considered unlikely to cause the US-induced lung haemorrhage. Thus, the alveolar resonance mechanism have not been proved or disproved.

## 2.1.5 The Alveoli

### 2.1.5.1 Function of Alveoli

The alveoli in the lungs function as a gas exchanger between the air and blood. The pulmonary capillaries of the alveoli exchanges  $\text{CO}_2$  for  $\text{O}_2$  from the air in the alveolar spaces through pressure diffusion (Figure 2.2).

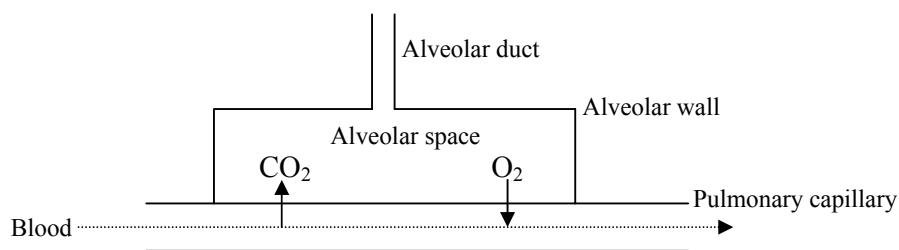


Figure 2.2: The alveolus as the pulmonary gas exchanger.

Hence naturally, the alveoli are engineered to have high density of gas exchange surface in order to facilitate diffusion of O<sub>2</sub> into the capillaries (Weibel ER, 2008). The functional importance of alveoli depends on the design of its walls, its surface area and its provision with parenchyma capillaries (Weibel ER & Gomez DM, 1962).

#### **2.1.5.2 Structure of Alveolus**

In mammals, the trachea (lung airway) branches into two bronchi and these then subdivides and branches into bronchioles. The bronchioles further subdivide through many levels and terminate with the alveoli (Slonim NB & Hamilton LH, 1987). The alveoli and its structure and characteristics are basically similar among mammalian species, albeit with some variations. The ratio of surface area of the pulmonary capillaries and alveolar spaces is ~1 (Harkema JR et al, 2000). All mammalian species have bronchioles interconnected to alveolar ducts. These alveolar ducts act as entrances to the alveoli (Mercer RR & Crapo JD, 1992).

The amount of smooth muscles that are present in the alveolar ducts varies with mammalian species (Tyler WS & Julian MD, 1992). In humans, pigs and monkeys; the smooth muscles extend past alveolar ducts while in mice, rats and rabbits; the smooth muscles terminate at bronchiole-alveolar duct junctions (Harkema JR et al, 2000). However, this structural difference in mammals is independent of the mechanism that causes US-induced lung haemorrhage (O' Brien Jr. WD et al, 2006). The resulting lesions are similar in morphology and character. The size of the alveolus and its wall thickness depend on the type of mammalian species. The US-

induced lung haemorrhage is dependent on these alveolar dimensions (Rott HD, 1997).

An alveolus is actually not spherical as according to popular misconception. It is in fact polygonal, which apparently is space-filling as to maximize surface area (Prange HD, 2003). In three-dimensional space, the typical alveolus resembles a polyhedral with 14-faceted pentagonal surfaces, with one open-end facet for the alveolar duct (Freed AD, 2012). The complex structure is usually represented as a dodecahedron (Karakaplan AD et al., 1980) as in Figure 2.3(a), and sometimes as a truncated octahedron (Dale PJ et al., 1980). The rhombic dodecahedron, made of twelve rhombus facets, was modelled as an alveolus by de Ryk J et al. (2007).

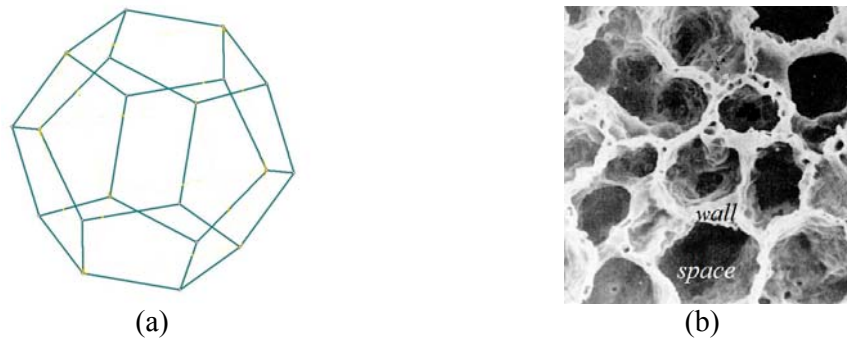


Figure 2.3: (a) The alveolus represented as a dodecahedron (MacLean KJM, 2007). (b) The arrangement pattern of the alveoli akin to froth or honeycomb (SRJC, 2013).

Structurally, the alveoli are typically bunched up together into alveolar sacs along the alveolar ducts. Thus, the alveoli are actually not discrete and separate elements but are interconnected with each other. Most alveoli share alveolar walls. Therefore, the alveoli resemble not as individual bubble spheres but are like froth or the honeycomb structure (Figure 2.3(b)) (Shields TW et al., 2009).

### 2.1.5.3 Alveolar Wall

The lung parenchyma contains collagens of mostly Type I and Type III that provide the structural framework and strength of the alveolar wall (Huang K et al., 2007). A gluing substance called proteoglycans embeds elastin fibres to the collagens, forming the extra-cellular matrix (ECM). Elastin fibres are mechanically connected to the collagens in order to provide elasticity. There are also some interstitial smooth muscles cells in the ECM, which furnish visco-elastic properties (Suki B et al., 2005). The alveolar wall is built on the foundation of the ECM.

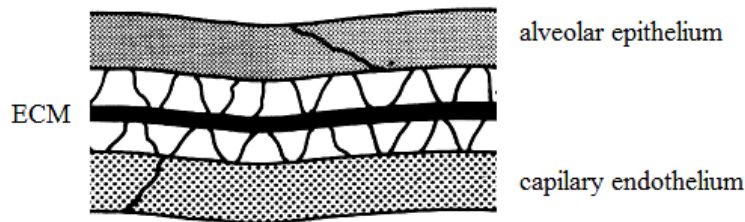


Figure 2.4: The BGB within an alveolar wall (West JB & Mathieu-Costello O, 1992).

In the alveolar wall, the capillaries within are arranged as a single layer separated from the air spaces by a thin cellular barrier known as the BGB. The BGB is made of the alveolar epithelium layer together with the capillary endothelium layer, as seen in Figure 2.4. The alveolar epithelium and the capillary endothelium layers are fused together by the ECM (Vaccaro CA & Brody JS, 1981). The BGB is relatively very thin (minimum thickness ~ 200 nm) and is susceptible to rupture due to its inability to expand significantly (Maina JN & West JB, 2005).

Alveolar walls are also penetrated by inter-alveolar pores which equalize the air pressure in alveoli. This causes the air pressures within the alveoli of different radii to be identical (Hill MJ et al., 1997). The density of alveolar wall, which is composed

of various types of mostly soft tissues, is approximated to range from 1026 – 1068 kg/m<sup>3</sup> (Ludwig GD, 1950). Meanwhile, the thickness of alveolar wall depends on the species of mammals.

#### **2.1.5.4 Strain in Alveolar Wall**

The integrity of the lung parenchyma structure is ensured by the tension of the ECM continuum that supports the alveolar walls and pulmonary capillaries. Alveoli are; hence, held together in place by the connective ECM. Since alveoli share common borders or walls with each other, the resulting radial traction maintains omnidirectional tension which prevents the alveoli from collapsing (Mead J et al., 1970).

Fung YC (1975) and Andreassen S et al. (2010) state that the net tension of alveolar wall is the total of its surface tension and also its elastic tension. However, the maximum value of surface tension of the alveoli is 50 dynes/cm (0.05 Nm<sup>-1</sup>) and is relatively quite small (Jardins TRD, 2007).

The elastic tension of the alveolar wall is considerably larger as it depends on the strain caused by normal tidal breathing. During the inspiration of normal breathing, from 20% of the total lung capacity (TLC) onwards, the alveolus undergoes stretching (Carney DE et al., 1999). Hence, the linear strain in alveolar wall varies from 0 – 0.05 during the normal tidal breathing (Roan E & Waters CM, 2011). This range of strain will be utilized in this study as linear strain of tidal breath.

Belete HA et al. (2009) states that the wounding of cells in parenchyma tissue occurs significantly at linear strain value of 0.08. Vlahakis NE & Hubmayr RD (2000) also

summarized that an excess linear strain percentage of 2% to 3% (above the maximum linear strain of tidal breath of 0.05) is needed to form fractures in the endothelial and epithelial plasma membranes and cells of alveolar wall. Thus, this value of 0.08 is regarded as the total linear strain that can damage the components within the alveolar wall and cause lung haemorrhage. It will be known in this study as the yield linear strain.

### **2.1.6 Risk Indicators of Ultrasound Bioeffects**

The FDA of the United States of America regulates the acoustic output levels for the diagnostic US imaging system through output display standards. The output levels are quantified by using the indexes, MI and TI (thermal index) (AIUM/NEMA, 1992). The MI was originally developed as a relative indicator of the potential for mechanical bioeffect (Apfel RE & Holland CK, 1991). The MI of US exposure is defined as the derated peak rarefactional pressure (MPa) over the square root of the acoustic centre frequency (MHz) (de Jong N, 2002):

$$MI = P_{r.3} / f^{1/2} \quad (2.2)$$

The FDA regulations require the MI to be  $\leq 1.9$  and should be kept 'as low as reasonably achievable' (ALARA) when using the US as a diagnostic tool (Nelson TR et al, 2009). This is to prevent over-exposure and any detrimental bioeffects on humans. Past studies show that the MI is a better indicator of lung damage than the derated spatial peak pulse average intensity (ISPPA<sub>3</sub>) or the derated peak rarefactional pressure ( $P_{r.3}$ ), for the estimation of US-induced lesion threshold (O'Brien Jr WD & Zachery JF, 1997).

The difference between risk and hazard is that the risk is the probability of occurrences of harm and its severity, while hazard is defined as the possible source of harm. The effective dose for 5% incident risk of US-induced lung haemorrhage is denoted as ED<sub>05</sub> (Simpson DG et al., 2004). During comparison across animal species, the ED<sub>05</sub> is obtained even when the MI  $\leq$  1.9, which is under the FDA regulatory limit.

## **2.2 Theory**

### **2.2.1 Ultrasound Characteristics**

The US is essentially a longitudinal wave. The US waves propagate in a medium through the compression and rarefaction of the molecules of medium. Hence, the US wave is characterized by varying pressures. An US wave cycle can be represented as a graph of local pressure in the medium versus the distance of propagation (Hendee WR & Ritenour ER, 2002). The number of cycles per unit time is the frequency of the US wave. The US is basically sound waves that exceed the upper limit of audible human hearing of 20 kHz. Medical US uses waves above 1 MHz. The distance of a wave cycle is known as the wavelength. The frequency ( $f$ ) and wavelength ( $\lambda$ ) of the US are inversely related by the speed of the longitudinal US waves as

$$c_L = f \cdot \lambda \quad (2.3)$$

In US equipments, the US waves are generated in pulses by piezoelectric transducers. These pulses consist of two or three sound cycles of the same US frequency. The number of pulses emitted is measured as the pulse repetition

frequency, which ranges from 1 – 10 kHz in medical US usage (Chan V & Perlas A, 2011). Meanwhile, the period of each pulse is known as pulse duration.

The maximum and minimum heights of the wave cycles, the amplitudes, are the US peak pressures (Jewett Jr JW & Serway RA, 2008). The US waves transports energy as it propagates through a medium. The intensity (energy per unit time per unit area) of the US waves, is measured as (Crocker MJ, 1998)

$$I = P_o^2 / 2\rho c_L \quad (2.4)$$

where  $P_o$  and  $c_L$  is the peak pressure and speed of the longitudinal US waves, respectively; while  $\rho$  is the density of the medium.

### 2.2.2 Propagation Modes of Waves

When a longitudinal wave impinges on the interface of two media, reflection and refraction can occur, as shown in Figure 2.5 (Lavender JD, 1976). The incident longitudinal wave ( $Li$ ) is reflected back as longitudinal wave ( $Lr$ ) and/or transverse wave ( $Tr$ ). The incident longitudinal wave (with angle  $\theta_{Li}$ ) can also be refracted as longitudinal wave ( $Lt$ ) and/or transverse wave ( $Tt$ ) with respective angles,  $\theta_{Lt}$  and  $\theta_{Tt}$ . Thus, the propagation mode of wave can be changed when longitudinal waves passes through layers of media.

The relation between the incident and refracted waves is obtained from the Snell's Law as (Rose JL, 1999)

$$\frac{\sin \theta_{Li}}{c_{Li}} = \frac{\sin \theta_{Lt}}{c_{Lt}} = \frac{\sin \theta_{Tt}}{c_{Tt}} \quad (2.5)$$

At a certain angle of incidence known as the critical angle, the refracted longitudinal wave propagates along the interface plane and hence is known as surface wave (S-wave).

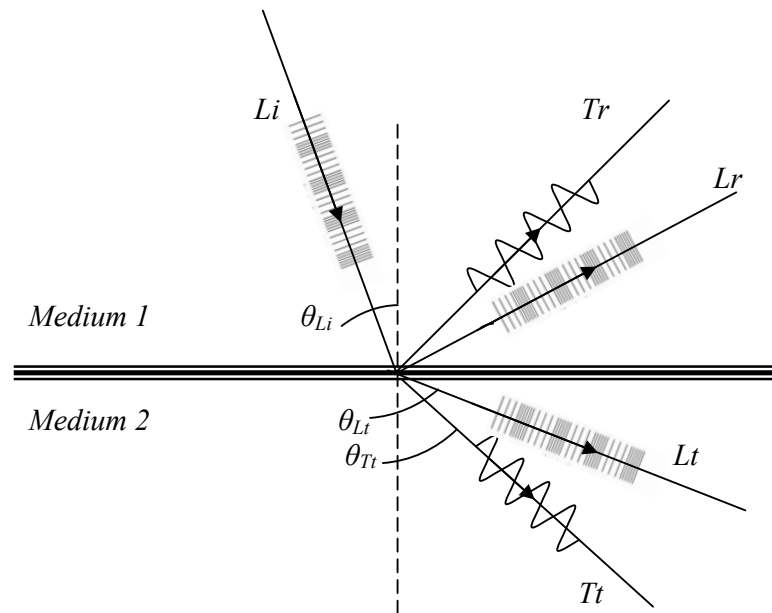


Figure 2.5: The incident longitudinal wave being reflected and refracted as longitudinal and transverse waves at the interface of media.

In the lungs, the interface is air-tissue. This interface of media can be regarded as fluid-fluid interface because soft tissues of parenchyma are incompressible alike liquid (Khaled W & Ermert H, 2008). The incidence of longitudinal wave at fluid-fluid interface produces only reflected and refracted longitudinal waves (Nagy PB, 2001). Therefore, the only propagation mode of waves in lungs when exposed to the US longitudinal waves is longitudinal only.